Thermonuclear ^{30}S$(p, \gamma)^{31}$Cl reaction in type I x-ray bursts

C. Wrede,[1,2,*] J. A. Caggiano,[3,†] J. A. Clark,[1,‡] C. M. Deibel,[1,‡] A. Parikh,[1,§] and P. D. Parker[1]

[1]*Wright Nuclear Structure Laboratory, Yale University, New Haven, Connecticut 06520, USA*

[2]*Department of Physics, University of Washington, Seattle, Washington 98195, USA*

[3]*TRIUMF, Vancouver, British Columbia V6T 2A3, Canada*

(Received 21 December 2008; revised manuscript received 3 March 2009; published 23 April 2009)

In the explosive astrophysical environment of a type I x-ray burst, the low Q value of 293(50) keV for proton capture on ^{30}S induces a $(p, \gamma)(\gamma, p)$ equilibrium that may lead to a waiting point in the rapid proton capture (rp) process at ^{30}S. The excitation energies of the first and candidate second $T = 3/2$ levels in ^{31}S were recently determined to an uncertainty of 2 keV by measuring triton spectra and t-p angular correlations from the ^{31}P(^{3}He, t)^{31}S$^*(p)^{30}$P reaction. By using this new information together with existing experimental information on the first $T = 3/2$, $A = 31$ isobaric multiplet and the isobaric multiplet mass equation, the ^{30}S$(p, \gamma)^{31}$Cl Q value is predicted to be 284(7) keV. Similarly, by using the second $T = 3/2$ multiplet, the energy of the dominant resonance in the thermonuclear ^{30}S$(p, \gamma)^{31}$Cl reaction is tentatively predicted to be $E_{\text{c.m.}} = 453(8)$ keV and this supports a ^{31}Ar β^+-delayed proton-decay observation of this resonance at $E_{\text{c.m.}} = 461(15)$ keV. These substantial reductions in the uncertainties in the thermonuclear ^{30}S$(p, \gamma)^{31}$Cl reaction rate and Q value constrain the region of temperature-density-composition parameter space where the ^{30}S$(p, \gamma)(\gamma, p)$ equilibrium and the ^{30}S waiting point may be active.

DOI: 10.1103/PhysRevC.79.045808 PACS number(s): 26.50.+x, 98.70.Qy, 21.10.Dr, 27.30.+t

I. INTRODUCTION

A type I x-ray burst (XRB) occurs when the hydrogen-rich envelope of an accreting neutron star undergoes a thermonuclear runaway. In this explosive environment, it is thought that the majority of rapid proton capture (rp) process nucleosynthetic flow passes through ^{30}S en route to heavier nuclear species [1]. This nuclide has been considered to be an rp-process waiting-point nuclide because (a) the low ^{30}S$(p, \gamma)^{31}$Cl Q value of 293(50) keV [2] establishes a $(p, \gamma)(\gamma, p)$ equilibrium [3] that is weighted toward ^{30}S at sufficiently high temperatures [1], (b) the half-life for β^+ decay of ^{30}S [terrestrial $t_{1/2} = 1.178(5)$ s] is comparable to burst-rise time scales of a few seconds, and (c) the competing ^{30}S$(\alpha, p)^{33}$Cl reaction is expected to be inhibited by the Coulomb barrier below $T \approx 1$ GK (typical peak XRB temperatures range from 1 to 2 GK) [1,4]. The interplay between the ^{30}S$(p, \gamma)^{31}$Cl$(\gamma, p)^{30}$S equilibrium, the ^{30}S$(\beta^+\nu_e)^{30}$P decay, and the ^{30}S$(\alpha, p)^{33}$Cl reaction may, therefore, influence the burst profile. Indeed, the ^{30}S waiting point and a similar waiting point at ^{34}Ar have been proposed [4] to explain observations of double-peaked XRB luminosity curves [5–8]. The 50-keV uncertainty in the ^{30}S$(p, \gamma)^{31}$Cl Q value results in large variations in the threshold temperatures for the ^{30}S waiting point and this could, in turn, affect the path and rate of nuclear flow to heavier species [9]. Uncertainty in this Q value is dominated by the uncertainty in the single measurement [10] of the ^{31}Cl$_{\text{g.s.}}$ mass excess. Additionally, uncertainties and inconsistencies in estimates of the thermonuclear ^{30}S$(p, \gamma)^{31}$Cl reaction rate result in a large uncertainty in the threshold temperatures for ^{30}S$(p, \gamma)^{31}$Cl$(\gamma, p)^{30}$S equilibrium—a prerequisite for the waiting point. The properties of the first excited state in ^{31}Cl are expected to determine the resonant ^{30}S$(p, \gamma)^{31}$Cl reaction rate. An observation [11] of this level in the β^+-delayed proton decay of ^{31}Ar needs to be confirmed and acknowledged in an astrophysical context.

In the stellar environment of an XRB, the nuclei involved in the explosion are nondegenerate and their nonrelativistic kinetic energies may be described by a Maxwell-Boltzmann distribution characterized by temperature T. The resonant ^{30}S$(p, \gamma)^{31}$Cl reaction rate per particle pair [12] is given by a sum over narrow, isolated resonances r,

$$\langle \sigma \upsilon \rangle = \left(\frac{2\pi}{\mu k_b T} \right)^{3/2} \hbar^2 \sum_r (\omega\gamma)_r e^{-E_r/k_b T}, \tag{1}$$

where $\hbar$ is the reduced Planck constant, k_b is the Boltzmann constant, μ is the reduced mass, and E_r is the resonance energy in the c.m. frame. The factor

$$(\omega\gamma)_r = \frac{(2J_r + 1)}{(2J_p + 1)(2J_S + 1)} \left(\frac{\Gamma_p \Gamma_\gamma}{\Gamma} \right)_r \tag{2}$$

in each term is the resonance strength, where $J_p(= 1/2)$, $J_S(= 0)$, and J_r are the spins of the reactants and the resonance, respectively. Γ_p and Γ_γ are the proton and γ-ray partial widths of the resonance, respectively, and $\Gamma = \Gamma_p + \Gamma_\gamma$ is the total width. Each term in the sum in Eq. (1) has an exponential dependence on E_r because of the Coulomb barrier. Nonresonant, direct proton-capture contributions to the

*wrede@u.washington.edu

†Present address: Pacific Northwest National Laboratory, Richland, WA 99352, USA.

‡Present address: Physics Division, Argonne National Laboratory, Argonne, IL 60439, USA.

§Present address: Physik Department E12, Technische Universität München, D-85748 Garching, Germany.

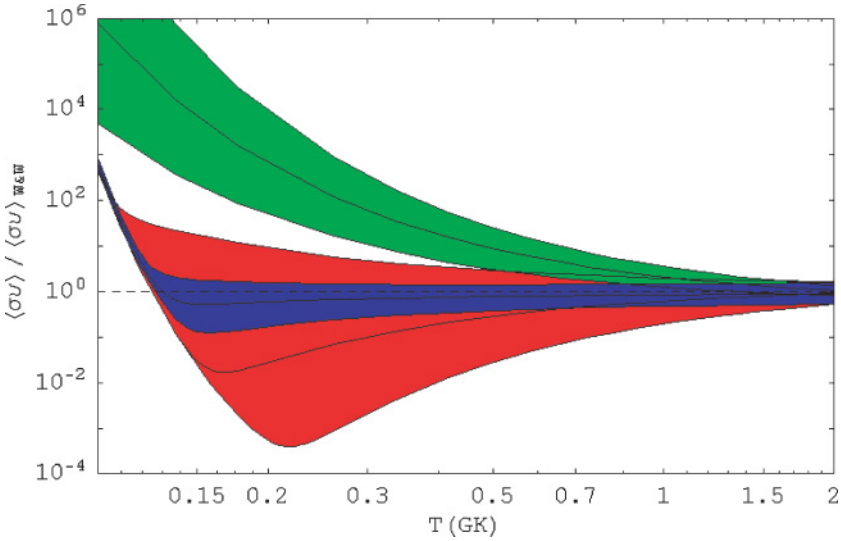

FIG. 1. (Color online) Ratio of the $^{30}S(p,\gamma)^{31}Cl$ reaction rate from the present work (darkest shade; blue online), Herndl *et al.* [13] (medium shade; red online), and Iliadis *et al.* [15] (lightest shade; green online) to that of Wallace and Woosley [14] (dashed). The uncertainty bands for the rate from the present work represent the total uncertainty in the rate. The uncertainty bands for the rate from Ref. [13] represent only the uncertainty in the rate derived using the upper and lower uncertainty limits on E_r. The uncertainty bands for the rate from Ref. [15] represent only the uncertainty in the rate derived using the upper and lower uncertainty limits on the DC component and E_r of the first resonance.

reaction rate are also expected to be important at the lowest stellar temperatures [13].

The initial evaluation of the thermonuclear $^{30}S(p,\gamma)^{31}Cl$ reaction rate was made by Wallace and Woosley [14], who simply predicted the first excited state of ^{31}Cl to lie at the same excitation energy as the first excited state of its mirror, ^{31}Si, yielding a resonance energy of $E_r = 453$ keV; the authors did not assign an uncertainty to this value. Subsequently, Herndl *et al.* [13] used shell-model calculations to predict $E_r = 520$ keV and make new estimates of partial widths. These authors also added a direct proton-capture contribution to their rate calculation and considered the resonant contribution from the second excited state of ^{31}Cl, which they calculated to lie at $E_r = 1470$ keV. A comparison of the excitation-energy calculations in Ref. [13] to measured values for a variety of nuclei showed that the uncertainty in the calculations is $\lesssim$100 keV. The net result was a lower reaction rate than that in than Ref. [14] (except at temperatures below 0.12 GK where direct capture dominated). Most recently, Iliadis *et al.* [15] used the isobaric multiplet mass equation (IMME) to predict $E_r = 330(45)$ keV for the energy of the first resonance based on data from Ref. [16]. These authors also re-examined the $^{36}Ar(^3He,^8Li)^{31}Cl$ spectra published in Ref. [10] and found evidence for the second excited state of ^{31}Cl, which they estimated to correspond to a $^{30}S + p$ resonance energy of $E_r \approx 1109$ keV. Because of the dramatically lower resonance energies deduced, the reaction rate given in Ref. [15] was up to five orders of magnitude higher than those in Refs. [13,14]. Ratios of the three reaction rates in Refs. [13–15] to that in Ref. [14] are plotted as functions of stellar temperature in Fig. 1. In Secs. II and III of the present work, updated experimental data on the $A = 31$, $T = 3/2$ isobaric multiplets are used together with the IMME to constrain the $^{30}S(p,\gamma)^{31}Cl$ reaction rate and Q value. The effects of these new values on the ^{30}S waiting point are then examined in Sec. IV.

II. $A = 31$, $T = 3/2$ ISOBARIC MULTIPLET MASS EQUATION: STATUS AND UPDATE

Under isospin symmetry [17] isobaric analog states (IAS) would be degenerate. In reality, charge-dependent interactions break isospin symmetry and the degeneracy of IAS. By applying a first-order perturbation of two-body Coulomb interactions to the nuclear Hamiltonian and incorporating the neutron-proton mass difference, one may derive the quadratic IMME [18,19],

$$\Delta(T_z) = a + bT_z + cT_z^2, \tag{3}$$

which compactly parametrizes the mass excess Δ of an individual member of a given isobaric multiplet as a function of its isospin projection, $T_z = (N - Z)/2$. For $A > 9$, Eq. (3) has been shown to be a reliable predictor of nuclear masses after the coefficients have been determined empirically, provided the experimental input data are accurate [20,21]. One way to predict the mass excesses of the ground and first excited states of ^{31}Cl using the IMME is to fit Eq. (3) to the known mass excesses of the $-3/2 \leqslant T_z \leqslant 3/2$ members of their respective $T = 3/2$ quartets to determine the coefficients, and then evaluate Eq. (3) at $T_z = -3/2$ in each case. The mass excesses of the first two $T = 3/2$ levels in ^{31}Si and ^{31}P and the ground-state mass excess of ^{31}S are known to better than 2 keV [2,16,22]. The dominant uncertainties in the IMME predictions of the ^{31}Cl-level mass excesses of interest lie in the excitation energies of $T = 3/2$ ^{31}S levels.

Population of $T = 3/2$ ^{31}S levels is isospin forbidden in commonly studied [16,22] single-neutron removal reactions on $T = 0$ ^{32}S. The first ($J^\pi = 3/2^+$) and second ($J^\pi = 1/2^+$) $T = 3/2$ ^{31}S levels were discovered by Davidson *et al.* [23] to lie at $E_x = 6277(25)$ and 7006(25) keV, respectively, using the $^{29}Si(^3He, n)$ ^{31}S reaction, through which population of $T = 3/2$ ^{31}S levels is isospin allowed. A subsequent measurement [24] of the isospin-allowed $^{33}S(p,t)$ $^{31}S(T = 3/2)$ reaction determined the first $T = 3/2$ level to lie at $E_x = 6268(10)$ keV. More recently, Kankainen *et al.* [25] used the β^+-delayed γ decay of ^{31}Cl to measure its IAS at $E_x = 6280(2)$ keV. In nuclear-data compilations [22,26] the second $T = 3/2$ level from Ref. [23] was identified with a level observed in the $^{32}S(^3He, \alpha)$ ^{31}S reaction [27,28], apparently based on similar excitation energies, and this influenced the recommended energy and uncertainty to be $E_x = 6996(15)$ keV. However, Vernotte *et al.* [29] have pointed out that the

TABLE I. IMME input for first and second $A = 31$, $T = 3/2$ quartets. Square brackets denote values that are based upon the tentative assignment of the second $T = 3/2$ ^{31}S level in Ref. [32].

T_z	Nuclide	$\Delta_{g.s.}$ (keV)	First E_x (keV)	Second E_x (keV)	First Δ (keV)	Second Δ (keV)
3/2	^{31}Si	−22949.01(4)	0	752.43(10)	−22949.01(4)	−22196.58(11)
1/2	^{31}P	−24440.88(18)	6380.8(17)	7140.6(15)	−18060.1(17)	−17300.3(15)
−1/2	^{31}S	−19044.6(15)	6281.5(14)	[7036(2)]	−12763.1(21)	[−12008.6(25)]
−3/2	^{31}Cl	−7067(50)	0		−7067(50)	

^{32}S(^{3}He, α) ^{31}S($T = 3/2$) reaction is isospin forbidden. Those authors measured the ^{32}S(^{3}He, α) ^{31}S level in question to have $E_x = 6966(5)$ keV, and they considered it to have $T = 1/2$. The interpretation of Vernotte *et al.* is presently adopted. Population of the second $T = 3/2$ level via β^+ decay of ^{31}Cl *is* allowed by β-decay selection rules and energy considerations. Indeed, a ^{31}S level has been inferred at $E_x = 7006(30)$ [30] and 7015(19) keV [25] based on ^{31}Cl β^+-delayed proton decay measurements by assuming that the proton decay is to the ground state of ^{30}P. This oversimplified decay scheme prompted Endt to undo [22] his initial identification [16] of the level observed in β^+ decay with the second $T = 3/2$ level. The interpretation of Endt regarding this matter is adopted, although it is certainly possible that the second $T = 3/2$ level was being observed in the β^+-decay work. The IMME predictions in Ref. [15] were based upon the outdated excitation energy in Ref. [16], where the ^{32}S(^{3}He, α)^{31}S [27,28] and β^+-decay [30] level energies were averaged with the ^{29}Si(^{3}He, n)^{31}S level energy to yield $E_x = 6997(14)$ keV for the second $T = 3/2$ level. The excitation energies of the first and second $T = 3/2$ levels in ^{31}S are considered by the present authors to be 6280(2) and 7006(25) keV, respectively, prior to the present work because these are the most precise unambiguous measurements of these levels.

Population of $T = 3/2$ ^{31}S levels is isospin allowed in the ^{31}P(^{3}He, t) ^{31}S reaction, measured for the first time by the present authors [31,32]. The first $T = 3/2$ level was identified by its excitation energy, which was measured to be 6283(2) keV (consistent with Ref. [25]). The strongest candidate for the second $T = 3/2$ level was identified by (a) the expectation that the nonselective ^{31}P(^{3}He, t) ^{31}S reaction will populate it, (b) the proximity of the measured excitation energy of $E_x = 7036(2)$ keV to that from previous work [23], (c) the difference in energy between the first and second $T = 3/2$ levels in ^{31}Si and ^{31}P, and (d) the observation of an $\ell = 0$ t-p angular correlation in its proton decay to the $J^\pi = 1^+$, $T = 0$ ground state of ^{30}P, consistent with $J^\pi(^{31}\text{S}^*) = 1/2^+$. Such isospin-forbidden decays are not uncommon [33,34] in cases where the proton decay only needs to compete with γ decay. Weighted averages of precision ($\leqslant$2-keV uncertainty) measurements yield $E_x = 6281.5(14)$ keV [25,31] and $E_x =$ [7036(2)] keV [32] for the first two $T = 3/2$ ^{31}S levels. (Square brackets are used to denote numbers that are based upon the tentative assignment of the second $T = 3/2$ ^{31}S level in Ref. [32].)

These new ^{31}S values are used together with the previously measured $A = 31$, $T = 3/2$ mass excesses to determine the coefficients in Eq. (3) using a least-squares fit. By using these coefficients, the mass excesses of the ground and first excited states of ^{31}Cl are predicted to be −7058(7) and [−6322(7)] keV, respectively, where the uncertainties have been rounded upward to the nearest keV. The IMME input values are summarized in Table I; the output coefficients and mass excesses are summarized in Table II.

III. ^{30}S(p, γ)^{31}Cl REACTION

A. Thermonuclear rate

The predicted ^{31}Cl first excited state mass excess may be used to calculate the corresponding ^{30}S(p, γ)^{31}Cl resonance energy, $E_r = \Delta(^{31}\text{Cl}^*) - \Delta(^{30}\text{S}) - \Delta(^1\text{H}) =$ [453(8)] keV, where the known ground-state mass excesses of ^{30}S and ^{1}H from Ref. [2] were used. This value may be compared to that derived from the E_p(laboratory) = 446(15)-keV peak observed in the ^{31}Ar β^+-delayed proton decay spectrum of Ref. [11], which yields a ^{30}S(p, γ)^{31}Cl resonance energy $E_r = 461(15)$ keV when transformed into the c.m. frame. The agreement between the prediction and the measurement is excellent. The potential observation of the first excited state of ^{31}Cl was explicitly discussed in Ref. [11] because this level is expected to have $J^\pi = 1/2^+$ and its direct population by the β^+ decay of $J^\pi = 5/2^{(+)}$ ^{31}Ar$_{g.s.}$ is second forbidden by β-decay selection rules. Indeed it would be unusual for a second-forbidden transition to occur in as many as 0.13% of ^{31}Ar β^+ decays when several allowed transitions exist. However, weak feeding of this level by the γ decay of higher lying ^{31}Cl levels that are directly populated by ^{31}Ar β^+ decay could also produce the observed results. The γ-ray detectors employed in that experiment were only sensitive to β^+-delayed γ rays at the $\approx$1% level and would not have been expected to detect ^{31}Cl de-excitation γ rays at the 0.1% level. Analogously, the $E_x = 752$ keV, $J^\pi = 1/2^+$ first excited state of ^{31}Si has been observed in the β^--delayed γ decay of $J^\pi = 5/2^+$ ^{31}Al [35]. This state (presumably the mirror of the level of interest in ^{31}Cl) was populated at the 6% level

TABLE II. IMME output for ^{31}Cl. Square brackets denote values that are based upon the tentative assignment of the second $T = 3/2$ ^{31}S level in Ref. [32].

	First quartet	Second quartet
a (keV)	−15462.6(15)	[−14703.9(15)]
b (keV)	−5296.9(27)	[−5291.7(29)]
c (keV)	204.0(20)	[197.7(20)]
$\Delta(T_z = -3/2)$ (keV)	−7058.2(62)	[−6321.5(64)]

TABLE III. Resonance parameters for the $^{30}S(p,\gamma)^{31}Cl$ reaction.

E_r (keV)	J^π	ℓ	Γ_γ (meV)	$\omega\gamma$ (meV)
461(15)	$1/2^+$	0	$0.86^{+0.60}_{-0.35}$	$0.86^{+0.60}_{-0.35}$
1462(5)	$5/2^+$	2	$0.80^{+0.56}_{-0.33}$	$2.4^{+1.7}_{-1.0}$

by the γ decay of a higher lying ^{31}Si state and possibly also at the 0.8% level by direct β^- decay from ^{31}Al. The present IMME prediction together with the other evidence discussed here supports the observation of the first excited state of ^{31}Cl in Ref. [11]. The measured value is adopted hereafter because the (more precise) IMME prediction is based on the *tentative* $T = 3/2$ assignment in ^{31}S.

The $^{30}S(p,\gamma)^{31}Cl$ resonant-reaction rate [Eq. (1)] is calculated by using an experimentally measured value [11] for the $^{30}S + p$ resonance energy of the first excited state of ^{31}Cl for the first time, $E_r = 461(15)$ keV. The second resonance is included in the calculation at a resonance energy of $E_r = 1462(5)$ keV, also deduced from ^{31}Ar β^+-decay measurements [11]. These resonance energies are both consistent with the shell-model predictions of Ref. [13] but are inconsistent with Ref. [15]. Following past work, it is assumed that $J^\pi = 1/2^+$ for the first resonance and $J^\pi = 5/2^+$ for the second resonance. These J^π assignments are supported by shell-model calculations [13], mirror levels in ^{31}Si, and the IMME. Values for Γ_γ are adopted directly from the measured lifetimes of the ^{31}Si mirror levels [16]; the γ-ray energy dependencies are neglected owing to their small effects. An uncertainty of a factor of 1.7 is assumed for both γ-ray partial widths based on mirror-level comparisons in the $21 \leqslant A \leqslant 44$ mass region [36]. This assumption should hold for the lower lying resonance, whose mirror decays by a transition with a tentatively assigned multipolarity of $M1$ [22]. The decay of the mirror to the higher lying resonance is known to be dominated by a mixed $M1 + E2$ transition [22] so the assumption is weaker in this case. However, it will be shown that the higher lying resonance makes a very minor contribution to the total rate, so this uncertainty is not critical. An estimation of Γ_p is not required since $\Gamma_\gamma\Gamma_p/\Gamma \approx \Gamma_\gamma$ under the reasonable assumption that $\Gamma_p \gg \Gamma_\gamma$ for both resonances. Resonance parameters are summarized in Table III. The direct-capture (DC) component of the reaction rate was calculated using Eq. (3.94) from Ref. [12] by adopting the constant astrophysical S factor of 5.14 keV b from Ref. [13] and the atomic masses from Ref. [2]. A 30% uncertainty is assumed for the present DC rate based on Ref. [15].

The sum of the DC rate and the resonant rate is tabulated in Table IV and compared with previous evaluations in Fig. 1, which shows the present evaluation to be in good agreement with Refs. [13,14] and poor agreement with Ref. [15] owing to the different values of E_r used for the $1/2^+$ resonance. Direct capture is found to dominate the reaction rate for temperatures below 0.13 GK. At all other XRB temperatures the $J^\pi = 1/2^+$ resonance dominates. The $J^\pi = 5/2^+$ resonance and the DC each make a small contribution of $\approx$1% to the total rate at the highest XRB temperature of 2 GK. The uncertainty limits for the present rate are derived by adding contributions from the resonance energies, the resonance strengths, and the DC component in quadrature. Uncertainties in the resonance strengths were not estimated in Refs. [13,15] and therefore only the contributions from the resonance-energy uncertainties are shown in Fig. 1 for those cases. For similar reasons, the DC uncertainty is omitted for the case of Ref. [13] and the $J^\pi = 5/2^+$ resonance-energy uncertainty is omitted for the case of Ref. [15]. This procedure underestimates the overall uncertainties in the rates from Refs. [13,15], particularly at the highest temperatures, and also at the lowest temperatures for Ref. [13]. Figure 1 shows the considerable reduction in the reaction-rate uncertainty resulting from the present work, which is due primarily to the reduction in the uncertainty of the $J^\pi = 1/2^+$ resonance energy.

B. Q value

The predicted $^{31}Cl_{g.s.}$ mass excess of $-7058(7)$ keV is in agreement with the (adjusted [37]) previously measured [10] value of $-7067(50)$ keV. By using the present value together with the known masses of ^{30}S and ^{1}H [2], the $^{30}S(p,\gamma)^{31}Cl$ Q value is calculated to be 284(7) keV. This is a substantial improvement in precision over the Q value of 293(50) keV [2] deduced directly from the mass values of ^{1}H, ^{30}S, and ^{31}Cl. The IMME value is adopted because it is based on solid $T = 3/2$ assignments and is more precise than the measured value.

IV. IMPLICATIONS FOR TYPE I X-RAY BURSTS

In this section, the implications of the new $^{30}S(p,\gamma)^{31}Cl$ reaction rate and Q value on the ^{30}S waiting point in XRBs are discussed. A significant waiting point is established when several conditions are met. First, the time scales for (p,γ) and (γ,p) reactions between ^{30}S and ^{31}Cl must be shorter than the time scale for temperature change. Second, the time scales for reactions between ^{30}S and ^{31}Cl must be shorter than the time scales for destruction of ^{30}S and ^{31}Cl by other reactions and decays. Third, more than $\approx$20% of the nucleosynthetic flow must wait at ^{30}S for a time comparable to the time scale of the XRB. The first two conditions are the conditions for $^{30}S(p,\gamma)^{31}Cl(\gamma,p)^{30}S$ equilibrium [12], ensuring that the net abundance flow between ^{30}S and ^{31}Cl is roughly zero. The third condition is suggested in Ref. [1] to define a waiting point with the capability of influencing the observed XRB luminosity curve.

The first two conditions may be examined together. The time scale for temperature change during the burst rise is $\approx$1 s [1,38,39], and the time scale for reactions and decays leading out of the $(p,\gamma)(\gamma,p)$ cycle is dominated by the β^+ decays of ^{30}S (with mean lifetime $\tau_\beta \approx 1.59$ s under XRB conditions [1]) and ^{31}Cl (with mean lifetime $\tau_\beta \approx 0.389$ s under XRB conditions [1]). For comparison, the mean lifetime for destruction of a ^{30}S nucleus via the (p,γ) reaction in an astrophysical environment with density ρ and hydrogen mass fraction X_H is [12]

$$\tau_{p\gamma} = \left(\rho \frac{X_H}{M_H} N_A \langle \sigma \upsilon \rangle\right)^{-1}, \quad (4)$$

TABLE IV. Thermonuclear $^{30}S(p,\gamma)^{31}Cl$ reaction rate $N_A\langle\sigma\upsilon\rangle_{g.s.}$ in units of cm^3 mol^{-1} s^{-1} as a function of typical XRB temperatures T. N_A is Avogadro's number. The second column shows the direct capture (DC) contribution to the rate. Resonant capture (RC) contributions to individual resonances are denoted by J^π. The column labeled "Total RC + DC" is the recommended rate, and the final two columns are the rates at the "Low" and "High" uncertainty limits, respectively.

T (GK)	DC	$1/2^+$ RC	$5/2^+$ RC	Total RC + DC	Low	High
0.01	2.72×10^{-45}			2.72×10^{-45}	1.90×10^{-45}	3.43×10^{-45}
0.015	1.36×10^{-38}			1.36×10^{-38}	9.49×10^{-39}	1.76×10^{-38}
0.02	2.27×10^{-34}			2.27×10^{-34}	1.59×10^{-34}	2.95×10^{-34}
0.03	4.44×10^{-29}			4.44×10^{-29}	3.11×10^{-29}	5.78×10^{-29}
0.04	9.61×10^{-26}			9.61×10^{-26}	6.72×10^{-26}	1.25×10^{-26}
0.05	2.25×10^{-23}	4.18×10^{-43}		2.25×10^{-23}	1.58×10^{-23}	2.93×10^{-23}
0.06	1.44×10^{-21}	1.76×10^{-35}		1.44×10^{-21}	1.01×10^{-21}	1.87×10^{-21}
0.07	3.99×10^{-20}	4.77×10^{-30}		3.99×10^{-20}	2.78×10^{-20}	5.18×10^{-20}
0.08	6.15×10^{-19}	5.51×10^{-26}		6.15×10^{-19}	4.30×10^{-19}	7.99×10^{-19}
0.09	6.20×10^{-18}	7.78×10^{-23}		6.20×10^{-18}	4.34×10^{-18}	8.06×10^{-18}
0.10	4.54×10^{-17}	2.54×10^{-20}		4.54×10^{-17}	3.17×10^{-17}	5.90×10^{-17}
0.11	2.58×10^{-16}	2.85×10^{-18}		2.61×10^{-16}	1.83×10^{-16}	3.39×10^{-16}
0.12	1.20×10^{-15}	1.44×10^{-16}		1.35×10^{-15}	9.63×10^{-16}	1.99×10^{-15}
0.13	4.75×10^{-15}	3.94×10^{-15}		8.68×10^{-15}	5.06×10^{-15}	2.15×10^{-14}
0.14	1.64×10^{-14}	6.66×10^{-14}		8.30×10^{-14}	2.80×10^{-14}	2.73×10^{-13}
0.15	5.05×10^{-14}	7.67×10^{-13}		8.17×10^{-13}	2.03×10^{-13}	2.77×10^{-12}
0.16	1.41×10^{-13}	6.46×10^{-12}		6.61×10^{-12}	1.56×10^{-12}	2.15×10^{-11}
0.17	3.63×10^{-13}	4.22×10^{-11}		4.26×10^{-11}	1.04×10^{-11}	1.31×10^{-10}
0.18	8.70×10^{-13}	2.23×10^{-10}		2.24×10^{-10}	5.78×10^{-11}	6.55×10^{-10}
0.19	1.96×10^{-12}	9.81×10^{-10}		9.83×10^{-10}	2.69×10^{-10}	2.74×10^{-9}
0.20	4.16×10^{-12}	3.71×10^{-9}		3.72×10^{-9}	1.07×10^{-9}	9.97×10^{-9}
0.21	8.42×10^{-12}	1.23×10^{-8}		1.23×10^{-8}	3.73×10^{-9}	3.19×10^{-8}
0.22	1.63×10^{-11}	3.66×10^{-8}		3.66×10^{-8}	1.16×10^{-8}	9.15×10^{-8}
0.23	3.04×10^{-11}	9.86×10^{-8}		9.87×10^{-8}	3.24×10^{-8}	2.39×10^{-7}
0.24	5.46×10^{-11}	2.44×10^{-7}		2.44×10^{-7}	8.29×10^{-8}	5.76×10^{-7}
0.25	9.51×10^{-11}	5.60×10^{-7}		5.60×10^{-7}	1.96×10^{-8}	1.30×10^{-6}
0.26	1.61×10^{-10}	1.20×10^{-6}		1.20×10^{-6}	4.34×10^{-7}	2.71×10^{-6}
0.27	2.65×10^{-10}	2.43×10^{-6}		2.43×10^{-6}	9.03×10^{-7}	5.38×10^{-6}
0.28	4.26×10^{-10}	4.67×10^{-6}		4.68×10^{-6}	1.78×10^{-6}	1.01×10^{-5}
0.29	6.69×10^{-10}	8.57×10^{-6}		8.57×10^{-6}	3.33×10^{-6}	1.83×10^{-5}
0.30	1.03×10^{-9}	1.51×10^{-5}		1.51×10^{-5}	5.98×10^{-6}	3.17×10^{-5}
0.32	2.31×10^{-9}	4.17×10^{-5}		4.17×10^{-5}	1.72×10^{-5}	8.56×10^{-5}
0.34	4.85×10^{-9}	1.02×10^{-4}		1.02×10^{-4}	4.33×10^{-5}	2.04×10^{-4}
0.36	9.63×10^{-9}	2.24×10^{-4}		2.24×10^{-4}	9.79×10^{-5}	4.42×10^{-4}
0.38	1.82×10^{-8}	4.51×10^{-4}		4.51×10^{-4}	2.02×10^{-4}	8.76×10^{-4}
0.40	3.29×10^{-8}	8.45×10^{-4}	5.75×10^{-16}	8.45×10^{-4}	3.87×10^{-4}	1.62×10^{-3}
0.42	5.71×10^{-8}	1.48×10^{-3}	4.03×10^{-15}	1.48×10^{-3}	6.92×10^{-4}	2.81×10^{-3}
0.44	9.60×10^{-8}	2.47×10^{-3}	2.36×10^{-14}	2.47×10^{-3}	1.17×10^{-3}	4.63×10^{-3}
0.46	1.56×10^{-7}	3.92×10^{-3}	1.18×10^{-13}	3.92×10^{-3}	1.89×10^{-3}	7.29×10^{-3}
0.48	2.48×10^{-7}	5.97×10^{-3}	5.14×10^{-13}	5.97×10^{-3}	2.91×10^{-3}	1.10×10^{-2}
0.50	3.82×10^{-7}	8.77×10^{-3}	1.99×10^{-12}	8.77×10^{-3}	4.33×10^{-3}	1.61×10^{-2}
0.55	1.03×10^{-6}	2.01×10^{-2}	3.77×10^{-11}	2.01×10^{-2}	1.02×10^{-2}	3.63×10^{-2}
0.60	2.47×10^{-6}	3.97×10^{-2}	4.33×10^{-10}	3.97×10^{-2}	2.05×10^{-2}	7.10×10^{-2}
0.65	5.40×10^{-6}	6.99×10^{-2}	3.38×10^{-9}	6.99×10^{-2}	3.68×10^{-2}	1.24×10^{-1}
0.70	1.09×10^{-5}	1.13×10^{-1}	1.95×10^{-8}	1.13×10^{-1}	6.00×10^{-2}	1.99×10^{-1}
0.75	2.07×10^{-5}	1.69×10^{-1}	8.85×10^{-8}	1.69×10^{-1}	9.11×10^{-2}	2.97×10^{-1}
0.80	3.71×10^{-5}	2.40×10^{-1}	3.30×10^{-7}	2.40×10^{-1}	1.31×10^{-1}	4.19×10^{-1}
0.85	6.34×10^{-5}	3.24×10^{-1}	1.05×10^{-6}	3.24×10^{-1}	1.78×10^{-1}	5.65×10^{-1}
0.90	1.04×10^{-4}	4.22×10^{-1}	2.92×10^{-6}	4.22×10^{-1}	2.33×10^{-1}	7.33×10^{-1}
0.95	1.65×10^{-4}	5.32×10^{-1}	7.27×10^{-6}	5.32×10^{-1}	2.96×10^{-1}	9.22×10^{-1}
1.00	2.52×10^{-4}	6.53×10^{-1}	1.64×10^{-5}	6.53×10^{-1}	3.65×10^{-1}	1.13×10^{0}
1.20	1.08×10^{-3}	1.21×10^{0}	2.11×10^{-4}	1.21×10^{0}	6.88×10^{-1}	2.08×10^{0}
1.40	3.45×10^{-3}	1.82×10^{0}	1.26×10^{-3}	1.82×10^{0}	1.04×10^{0}	3.12×10^{0}
1.60	8.94×10^{-3}	2.40×10^{0}	4.71×10^{-3}	2.41×10^{0}	1.39×10^{0}	4.12×10^{0}
1.80	1.99×10^{-2}	2.92×10^{0}	1.28×10^{-2}	2.95×10^{0}	1.72×10^{0}	5.01×10^{0}
2.00	3.97×10^{-2}	3.35×10^{0}	2.81×10^{-2}	3.42×10^{0}	2.01×10^{0}	5.79×10^{0}

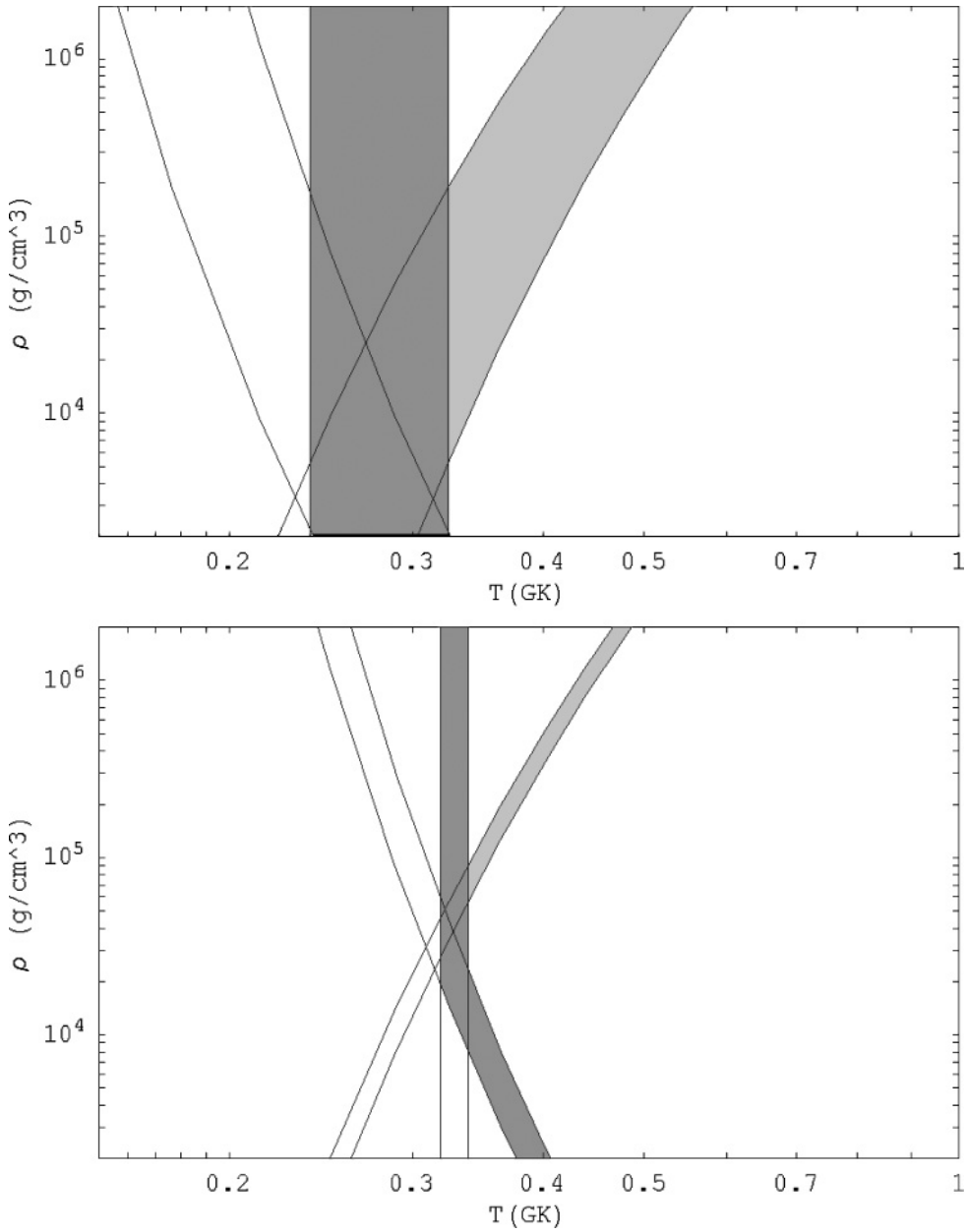

FIG. 2. Onset temperatures for $^{30}S(p,\gamma)^{31}Cl(\gamma,p)^{30}S$ equilibrium (dark shade) and the ^{30}S waiting point (light shade), using the most recent $^{30}S(p,\gamma)^{31}Cl$ reaction rate and Q value from Refs. [2,15] (top panel) and from the present work (bottom panel). The bands of negative slope are determined by the time scale for $^{30}S(p,\gamma)$ reactions, the vertical bands are determined by the time scale for $^{31}Cl(\gamma,p)$ reactions, and the bands of positive slope are determined by the condition that 20% of the nucleosynthetic flow must wait to pass through $^{30}S(\beta^+\nu_e)$. The width of each band is determined by the uncertainty limits on the rate and Q value. In both plots a hydrogen mass fraction of 0.75 is assumed.

where M_H is the atomic mass of hydrogen in atomic mass units. The mean lifetime for destruction of a ^{31}Cl nucleus via photodisintegration is [12]

$$\tau_{\gamma p} = \left(\frac{2\pi\hbar^2}{\mu kT}\right)^{3/2} \frac{(2J_{\rm Cl}+1)}{(2J_p+1)(2J_S+1)} \frac{G_{\rm Cl}}{G_S G_p} \frac{1}{\langle\sigma\upsilon\rangle} e^{Q/k_bT}, \tag{5}$$

where $J_{\rm Cl}(=3/2)$ is the spin of the ^{31}Cl ground state. The partition functions, G, of the reactant and product nuclides are all equal to unity for $T < 0.5$ GK [40]. By setting $\tau_{p\gamma} = 1$ s in Eq. (4) with a chosen reaction rate, a surface may plotted in T-ρ-X_H space that represents a low-temperature limit on the $^{30}S(p,\gamma)^{31}Cl(\gamma,p)^{30}S$ equilibrium based on ^{30}S. (The time scale for temperature change poses a more stringent constraint than that for β^+ decay of ^{30}S.) A similar surface based on ^{31}Cl may be plotted by setting $\tau_{\gamma p} = 0.389$ s in Eq. (5). (The time scale for β^+ decay of ^{31}Cl poses a more stringent constraint than that for temperature change.) Figure 2 shows the corresponding loci in T-ρ space for $X_H = 0.75$ (a typical value in XRBs) where the $^{30}S(p,\gamma)^{31}Cl(\gamma,p)^{30}S$-equilibrium threshold temperatures derived using the present reaction rate and Q value are compared to the temperatures derived using the reaction rate and Q value from Refs. [2,15]. Lower values of X_H shift the ^{30}S constraint to slightly higher temperatures and do not affect the ^{31}Cl constraint. In the relevant temperature range the reaction rate from the present work is orders of magnitude lower than that from Ref. [15] (Fig. 1), which raises the threshold temperatures for $^{30}S(p,\gamma)^{31}Cl(\gamma,p)^{30}S$ equilibrium; the uncertainties are also substantially reduced. It is possible that this result will delay the onset of, and reduce the duration of, the ^{30}S waiting point in XRBs.

The third condition is met when at least 20% of the reaction and decay flow out of ^{30}S must wait for its β^+ decay.

Neglecting the ^{31}Cl$(p,\gamma)^{32}$Ar and ^{30}S$(\alpha,p)^{33}$Cl reactions, which are very slow at the relevant temperatures [4,12], this condition may be written as

$$\lambda[^{30}\mathrm{S}(p,\gamma)^{31}\mathrm{Cl}(\beta^+\nu_e)] < 4\lambda[^{30}\mathrm{S}(\beta^+\nu_e)], \tag{6}$$

where $\lambda = 1/\tau$ are the decay constants for the processes in brackets. It can be shown [12] that under equilibrium conditions,

$$\frac{\lambda[^{30}\mathrm{S}(p,\gamma)^{31}\mathrm{Cl}(\beta^+\nu_e)]}{\lambda[^{31}\mathrm{Cl}(\beta^+\nu_e)]} = \frac{N^e_{\mathrm{Cl}}}{N^e_S} = \frac{\tau_{\gamma p}}{\tau_{p\gamma}}, \tag{7}$$

where N^e_S and N^e_{Cl} are the equilibrium abundances of ^{30}S and ^{31}Cl, respectively. By using Eqs. (4), (5), and (7) together with $\lambda = 1/\tau$ for ^{31}Cl$(\beta^+\nu_e)$, an expression can be found for $\lambda[^{30}\mathrm{S}(p,\gamma)^{31}\mathrm{Cl}(\beta^+\nu_e)]$. Using this expression together with $\lambda = 1/\tau$ for ^{30}S$(\beta^+\nu_e)$ and the inequality from Eq. (6) allows the threshold for the third waiting-point condition to be plotted (see Fig. 2) for $X_H = 0.75$ (with lower values of X_H shifting this condition to slightly lower temperatures). Because the ^{30}S$(p,\gamma)^{31}$Cl reaction rate cancels, this condition is primarily dependent on nuclear-physics data through the reaction Q value. Figure 2 shows the constraints imposed on the onset of the waiting point by the Q value from the present work in comparison to the Q value from Ref. [2]. An upper temperature limit of $\approx 1.0 \pm 0.3$ GK, representing the culmination point of the ^{30}S waiting point, is determined by the rate of the unmeasured ^{30}S$(\alpha,p)^{33}$Cl reaction [4].

V. CONCLUSIONS AND OUTLOOK

Acquiring further experimental information on the ^{30}S waiting point will be challenging, but new experiments could be used to test, or improve upon, the present findings. A precision measurement of the ^{31}Cl$_{\mathrm{g.s.}}$ ($t_{1/2} = 150$ ms) mass could be made using a Penning trap and could also be used to test the validity of the IMME itself for this multiplet. The mass excesses of ^{31}Cl levels could be measured to an uncertainty of better than $\approx$30 keV by using the ^{32}S(^{7}Li,^{8}He)^{31}Cl reaction and a magnetic spectrometer [41]. All resonance parameters could be measured directly if a radioactive ^{30}S-ion beam of sufficient intensity were available [4]. A beam of 10^8 ^{30}S ions/s would also enable direct measurements of the ^{30}S$(\alpha,p)^{33}$Cl reaction [4], which would determine the culmination temperatures for the ^{30}S waiting point more accurately. Finally, a high-resolution remeasurement of the ^{29}Si(^{3}He, n) reaction could be used to check the excitation energy of the second $T = 3/2$ level in ^{31}S.

In conclusion, precise excitation-energy measurements of the two $T_z = -1/2$ members of the lowest lying $T = 3/2$, $A = 31$ isobaric quartets have been used together with existing experimental data and the IMME to reduce uncertainties in the ^{30}S$(p,\gamma)^{31}$Cl Q value and the thermonuclear ^{30}S$(p,\gamma)^{31}$Cl reaction rate. By using this updated information the onset conditions for the ^{30}S rp-process waiting point in XRBs have been determined more precisely.

ACKNOWLEDGMENTS

Constructive comments from an anonymous referee are gratefully acknowledged. This work was supported by the U.S. Department of Energy, Office of Nuclear Physics, under Grant Nos. DE-FG02-91ER40609 and DE-FG02-97ER41020.

[1] J. L. Fisker, H. Schatz, and F.-K. Thielemann, Astrophys. J. Suppl. Ser. **174**, 261 (2008).
[2] G. Audi, A. H. Wapstra, and C. Thibault, Nucl. Phys. **A729**, 337 (2003).
[3] L. Van Wormer, J. Görres, C. Iliadis, M. Wiescher, and F.-K. Thielemann, Astrophys. J. **432**, 326 (1994).
[4] J. L. Fisker, F.-K. Thielemann, and M. Wiescher, Astrophys. J. Lett. **608**, L61 (2004).
[5] M. Sztajno, J. van Paradijs, W. H. G. Lewin, J. Trümper, G. Stollman, W. Pietsch, and M. van der Klis, Astrophys. J. **299**, 487 (1985).
[6] J. van Paradijs, M. Sztajno, W. H. G. Lewin, J. Trümper, W. D. Vacca, and M. van der Klis, Mon. Not. R. Astron. Soc. **221**, 617 (1986).
[7] W. Penninx, E. Damen, J. Tan, W. H. G. Lewin, and J. van Paradijs, Astron. Astrophys. **208**, 146 (1989).
[8] E. Kuulkers, J. Homan, M. van der Klis, W. H. G. Lewin, and M. Méndez, Astron. Astrophys. **382**, 947 (2002).
[9] A. Parikh, J. José, C. Iliadis, F. Moreno, and T. Rauscher, Phys. Rev. C (submitted).
[10] W. Benenson, D. Mueller, E. Kashy, H. Nann, and L. W. Robinson, Phys. Rev. C **15**, 1187 (1977).
[11] L. Axelsson, J. Äystö, M. J. G. Borge, L. M. Fraile, H. O. U. Fynbo, A. Honkanen, P. Hornshøj, A. Jokinen, B. Jonson, P. O. Lipas *et al.*, Nucl. Phys. **A634**, 475 (1998).
[12] C. Iliadis, *Nuclear Physics of Stars* (Wiley-VCH, Weinheim, 2007).
[13] H. Herndl, J. Görres, M. Wiescher, B. A. Brown, and L. Van Wormer, Phys. Rev. C **52**, 1078 (1995).
[14] R. K. Wallace and S. E. Woosley, Astrophys. J. Suppl. Ser. **45**, 389 (1981).
[15] C. Iliadis, J. M. D'Auria, S. Starrfield, W. J. Thompson, and M. Wiescher, Astrophys. J. Suppl. Ser. **134**, 151 (2001).
[16] P. M. Endt, Nucl. Phys. **A521**, 1 (1990).
[17] W. Heisenberg, Z. Phys. **77**, 1 (1932).
[18] E. P. Wigner, in *Proceedings of the Robert A. Welch Foundation Conference on Chemical Research, Houston*, edited by W. O. Millikan (Robert A. Welch Foundation, Houston, 1957), Vol. 1, p. 88.
[19] S. Weinberg and S. B. Treiman, Phys. Rev. **116**, 465 (1959).
[20] J. Britz, A. Pape, and M. S. Antony, At. Data Nucl. Data Tables **69**, 125 (1998).
[21] S. Triambak, A. García, E. G. Adelberger, G. J. P. Hodges, D. Melconian, H. E. Swanson, S. A. Hoedl, S. K. L. Sjue, A. L. Sallaska, and H. Iwamoto, Phys. Rev. C **73**, 054313 (2006).
[22] P. M. Endt, Nucl. Phys. **A633**, 1 (1998); http://www.nndc.bnl.gov/ensdf/.
[23] J. M. Davidson, D. A. Hutcheon, D. R. Gill, T. Taylor, D. M. Sheppard, and W. C. Olsen, Nucl. Phys. **A240**, 253 (1975).

[24] H. Nann and B. H. Wildenthal, Phys. Rev. C **19**, 2146 (1979).
[25] A. Kankainen, T. Eronen, S. P. Fox, H. O. U. Fynbo, U. Hager, J. Hakala, J. Huikari, D. G. Jenkins, A. Jokinen, S. Kopecky *et al.*, Eur. Phys. J. A **27**, 67 (2006).
[26] P. M. Endt and C. van der Leun, Nucl. Phys. **A310**, 1 (1978).
[27] F. Ajzenberg-Selove and J. L. Wiza, Phys. Rev. **143**, 853 (1966).
[28] T. S. Bhatia, W. W. Daehnick, and G. J. Wagner, Phys. Rev. C **5**, 111 (1972).
[29] J. Vernotte, G. Berrier-Ronsin, S. Fortier, E. Hourani, A. Khendriche, J. M. Maison, L.-H. Rosier, G. Rotbard, E. Caurier, and F. Nowacki, Nucl. Phys. **A655**, 415 (1999).
[30] J. Aysto, X. J. Xu, D. M. Moltz, J. E. Reiff, J. Cerny, and B. H. Wildenthal, Phys. Rev. C **32**, 1700 (1985).
[31] C. Wrede, J. A. Caggiano, J. A. Clark, C. Deibel, A. Parikh, and P. D. Parker, Phys. Rev. C **76**, 052802(R) (2007).
[32] C. Wrede, J. A. Caggiano, J. A. Clark, C. M. Deibel, A. Parikh, and P. D. Parker, Phys. Rev. C **79**, 045803 (2009).
[33] E. G. Adelberger, A. B. McDonald, C. L. Cocke, C. N. Davids, A. P. Shukla, H. B. Mak, and D. Ashery, Phys. Rev. C **7**, 889 (1973).
[34] J. F. Wilkerson, R. E. Anderson, T. B. Clegg, E. J. Ludwig, and W. J. Thompson, Phys. Rev. Lett. **51**, 2269 (1983).
[35] C. Détraz, D. Guillemaud, G. Huber, R. Klapisch, M. Langevin, F. Naulin, C. Thibault, L. C. Carraz, and F. Touchard, Phys. Rev. C **19**, 164 (1979).
[36] C. Iliadis, P. M. Endt, N. Prantzos, and W. J. Thompson, Astrophys. J. **524**, 434 (1999).
[37] A. H. Wapstra, G. Audi, and C. Thibault, Nucl. Phys. **A729**, 129 (2003).
[38] H. Schatz, A. Aprahamian, V. Barnard, L. Bildsten, A. Cumming, M. Ouellette, T. Rauscher, F.-K. Thielemann, and M. Wiescher, Phys. Rev. Lett. **86**, 3471 (2001).
[39] O. Koike, M. Hashimoto, R. Kuromizu, and S. Fujimoto, Astrophys. J. **603**, 242 (2004).
[40] T. Rauscher and F.-K. Thielemann, At. Data Nucl. Data Tables **79**, 47 (2001).
[41] J. A. Caggiano, D. Bazin, W. Benenson, B. Davids, R. Ibbotson, H. Scheit, B. M. Sherrill, M. Steiner, J. Yurkon, A. F. Zeller *et al.*, Phys. Rev. C **64**, 025802 (2001).